Cell
PRESS

Where does amantadine bind to the influenza virus M2 proton channel?

Dima Kozakov, Gwo-Yu Chuang, Dmitri Beglov and Sandor Vajda

Department of Biomedical Engineering, Boston University, 44 Cummington Street, Boston, MA 02215, USA

Structures of the influenza A virus M2 proton channel in the open conformation have been determined by X-ray crystallography, and in the closed conformation by NMR. Whereas the X-ray structure shows a single inhibitor molecule in the middle of the channel, four inhibitor molecules bind the channel's outer surface in the NMR structure. In both structures, the strongest hot spots (i.e., regions that contribute substantially to the free energy of binding any potential ligand) lie inside the pore, and other hot spots are found at exterior locations. By considering all available models, we propose the primary drug binding site is inside the pore, but that exterior binding occurs under appropriate conditions.

The amantadine binding controversy

The integral membrane protein M2 of influenza virus forms an acid-activated, proton-conducting ion channel that functions during viral uncoating and maturation by modifying the pH in virions as well as in trans-Golgi vesicles [1,2]. The low pH (5.5 – 6.0) of the endosome activates the M2 channel before hemagglutinin-mediated fusion. Proton conductance acidifies the viral interior, thereby facilitating dissociation of the matrix protein from the viral nucleoproteins, a process required for unpacking the viral genome [1]. The channel is highly selective for protons and has low permeability for other physiological ions according to reversal potential studies [3].

M2 is a 97 residue single-pass membrane protein with 23 amino acids of the N-terminus oriented extracellularly, a single internal hydrophobic domain of 19 residues that acts as the transmembrane domain (M2TM), and a 54 residue cytoplasmic tail [4,5]. M2TM is the target of the anti-influenza drugs amantadine and its methyl derivative rimantadine. The two drugs have been recommended as the first line of defense for several years in order to reserve the only other class of anti-influenza drugs, the neuraminidase inhibitors, in the event of an epidemic. Recently, however, most influenza strains have developed resistance to amantadine and rimantadine [6]. In particular, the Ser31Asn substitution renders the virus highly resistant to amantadine inhibition, and the incidence of clinical isolates bearing this mutation has jumped from a small percentage to approximately 97% in recent years [6–8]. Thus, it is important to understand how amantadine binds, why resistance to the drug develops, and whether other compounds can be found that inhibit the M2 channel.

The first structure of the M2 channel was solved for residues 22–46 by solid-state NMR (ssNMR) in 2002 [9]. More recently, Stouffer et al. [10] used X-ray crystallography to determine the structure for the same residues with and without amantadine in the detergent octyl-β-D-glucopyranoside (OG). At the same time, Schnell and Chou [11] used NMR to determine the structure of the rimantadine-bound M2 peptide of residues 18–60 solubilized in dihexanoylphosphatidylcholine (DHPC) micelles at pH 7.5. Both X-ray crystallography and NMR confirmed that the channel is a pseudosymmetric tetramer with the membrane-spanning region forming a left-handed coiled coil, but the two structures disagree regarding the position of the bound inhibitor [12]. In the X-ray structure, a single amantadine molecule binds in the middle of the pore, surrounded by residues Val27, Ala30, Ser31 and Gly34 (Figure 1). By contrast, the NMR data show four rimantadine molecules bound to the lipid-exposed outer surface of the channel at the membrane boundary close to the cytoplasmic end of the helices, interacting with residues Asp44 and Arg45 (Figure 1).

Here, we review the various M2MT structures that have been published, showing that the X-ray and NMR structures represent two extremes in terms of the tilt angle of the transmembrane helices with respect to the central axis of the channel. We then use binding site analysis tools to identify the most important binding sites in the two structures. To our surprise, the results suggest that the two very different structures have fairly similar hot spots, both in the channel pore and on the outer surface. However, these hot spots occupy pockets that substantially differ in size between the two structures, resulting in the different amantadine binding modes observed experimentally. Considering the similarity of hot spots in the two structures, we propose that both binding modes are possible under appropriate conditions. Indeed, we argue that the assumption of only one binding mode leaves a number of observations unexplained.

The geometry of the M2TM channel

The X-ray structures obtained by Stouffer et al. [10] represent the open state of the channel [12], with the four helices forming a left-handed, parallel bundle that resembles a truncated cone, with the narrow amino-terminal end facing the exterior of the viral envelope. The N-terminal half of the channel has nearly exact 4-fold rotational symmetry; the helices are tilted by $35°±2°$ with respect to the central axis of the bundle, in good agreement with the range of 32–38° determined by various ssNMR

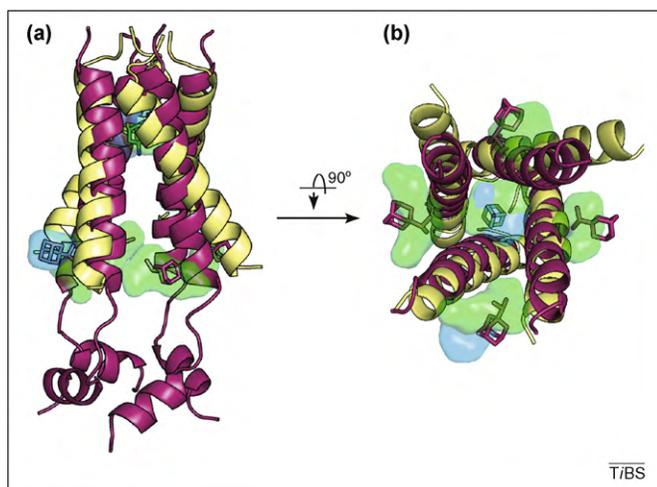*Corresponding author:* Vajda, S. (vajda@bu.edu).

Figure 1. Superimposition of the X-ray and the NMR structures of the truncated M2 proton channel. The proteins are shows as cartoons with the X-ray structure colored wheat and the NMR structure colored magenta. The amantadine bound in the middle of the channel in the X-ray structure is shown as green sticks. The four rimantadine molecules bound to the outer surface of the channel in the NMR structure are also shown in stick representation, colored magenta. The figures show the hot spot regions as transparent ''clouds'', colored light blue for the X-ray structure and light green for the NMR structure. **(a)** A side-view of the channel with the C-terminal cytoplasmic end of the channel located on the bottom. **(b)** View from the C-terminal cytoplasmic end. The C-terminal helices in the NMR structure are removed to show the channel's pore. Notice that the hot spots obtained for the two structures in the pore overlap with each other, and hence the region is shown in mixed colors. The two views also show that this hot spot is located at the amantadine binding site in the X-ray structure. For the NMR structure, the four hot spots on the outer surface overlap with the bound rimantadine molecule, and are visible on all four sides. By contrast, an external hot spot is visible only between two of the helices in the X-ray structure.

studies of both the open and closed states [9,13–17]. Although the NMR structure also shows that MTM2 is a four-helix bundle [11], the channel is in the closed conformation, and the tilt angle of the helices with respect to the lipid bilayer normal is only 23°, much smaller than that in the X-ray structure (Figure 1a).

Determining which of the two structures represents the biologically more relevant conformation is difficult for two main reasons. First, M2MT exhibits substantial plasticity and conformational heterogeneity, confirmed by both ssNMR and X-ray studies [17–22]. In particular, the transmembrane helix can be kinked around Gly34, and the kink angle can be changed by amantadine binding [17–19]. Nuclear spin relaxation data and polarization inversion spin exchange at the magic angle spectra revealed that the structure at high pH and in the absence of amantadine is more dynamic and structurally heterogeneous than the amantadine-bound structure [21]. This structural plasticity is suggested to be essential for channel opening, gating, and proton conduction [21]. A recent study using 1D and 2D IR spectroscopy indicates an even larger conformational change at neutral pH when the channel is closing [22]. The plasticity of the M2 channel was confirmed recently by molecular dynamics simulations [23–25].

The second factor that makes determining the structure of the M2TM channel difficult is its dependence on the experimental conditions [26]. Indeed, the tilt angle is influenced largely by sample preparation conditions such as solvents, membrane composition, peptide concentration, and particularly bilayer thickness [27–32]. In

particular, detergent micelles might cause curvature stress to membrane proteins, affecting their structure [29,30], and this is most likely responsible for the substantial difference between the X-ray and NMR structures. In fact, Chou *et al*. [29,30] noted that in the absence of the peptide, the DHPC micelle adopts a spherical shape with a diameter of 36 Å, whereas the length of the M2 transmembrane channel is only around 30 Å [11]. Thus, the channel appears to be stretched, and this might result in a tilt angle that is substantially smaller than that reported for the M2 channel in other biological membranes [13–20]. However, little information is available on micelle structure in the presence of a protein. For example, on the basis of intermolecular nuclear Overhauser effects (NOEs), Fernandez *et al*. [32] modeled DHPC molecules around a membrane protein oriented with their hydrophobic tails perpendicular to the hydrophobic protein surface, resulting in a distorted monolayer, and thus in an environment for the protein that differs substantially from the conditions in a natural lipid bilayer.

Analysis of the M2TM binding sites
The X-ray and the NMR structures represent two extremes in terms of the helical tilt angle, and hence it is interesting to determine the binding hot spots (i.e., the regions contributing substantially to the binding free energy) in both structures using computational solvent mapping (Box 1). In the X-ray structure, the top-ranked hot spot is located inside the channel at the amantadine binding site, interacting with amino acid residues Ser31, Val27, Ala30 and Gly34 (Figure 1). These residues form a large pocket [38], with a volume of 210 Å^3. The next three hot spots line the inside of the pore between residues Ile33 and His37, overlapping the water wire found in this part of the channel [33]. The fourth largest hot spot is located on the lipid-exposed outer surface of the channel (Figure 1), at the site that binds rimantadine in the NMR structure [11]. Probe binding to the outer surface occurs only between two helices, because the 35° tilt of the truncated helices yields large openings rather than pockets on the other three sides of the four-helix bundle. However, we expect to find four pockets for a structure with slightly longer peptides.

The mapping of the NMR structure yields interesting results. Although the NMR data [11] show four rimantadine molecules bound on the outside of the protein, the largest hot spot is within the pore near residues Ala30, Ser31, and Gly34, which line the amantadine binding site in the X-ray structure (Figure 1). The four next highest ranked hot spots are located on the outside of the channel at the rimantadine binding sites (Figure 1). In this structure, the four external sites (with volumes between 390 Å^3 and 190 Å^3) are the largest pockets, much larger than the internal site, which has a volume of only 85 Å^3. We note that probe binding at these sites is due, in part, to the favorable electrostatic interactions between the partially polar probes and the interfacial region of the lipid bilayer [33]. Indeed, the concentration of amantadine is much higher in this interfacial region than it is in the middle of the membrane [39,40].

Mapping results show that both the X-ray and NMR structures have the strongest hot spot located in the

---

Box 1. Identification of binding hot spots by computational solvent mapping

The binding sites of proteins generally include smaller regions called hot spots, which are major contributors to the binding free energy, and hence are crucial to the binding of any ligand at that particular site [34]. In drug design applications, such hot spots can be identified by screening for the binding of fragment-sized organic molecules [34–37]. Because the binding of the small compounds is very weak, it is usually detected by nuclear magnetic resonance (structure–activity relationships (SAR) by NMR [36]) or by X-ray crystallography [37]. The results show that the hot spots of proteins bind a variety of small molecules, and that the fraction of the ''probe'' molecules binding to a particular site predicts the potential importance of the site and can be considered a measure of druggability [34,35]. Solvent mapping has been developed as a computational analogue of the NMR- and X-ray-based screening experiments [35]. The method places molecular probes, which are small organic molecules containing various functional groups, on a dense grid defined around the protein, finds favorable positions using empirical free energy functions, further refines the selected poses by free energy minimization, clusters the low-energy conformations, and ranks the clusters on the basis of the average free energy [37]. For the identification of hot spots, we generally use 16 probes (ethanol, isopropanol, tert-butanol, acetone, acetaldehyde, dimethyl ether, cyclohexane, ethane, acetonitrile, urea, methylamine, phenol, benzaldehyde, benzene, acetamide and N,N-dimethylformamide). To determine the hot spots, we identify consensus sites (i.e., regions on the protein where clusters of different probes overlap) and rank these sites in terms of the number of overlapping probe clusters [35]. The sites with the largest number of probe clusters are considered as predictions of binding hot spots. Applications to a variety of proteins show that the probes always cluster in important subsites of the binding site and the amino acid residues that interact with many probes also bind the specific ligands of the protein [34]. For the analysis of the M2TM domain, the general algorithm [35] was modified slightly to account for the membrane, which was modeled as a layer of low dielectric medium [33]. We have mapped both the unbound X-tray structure and the 15 NMR structures (PDB codes 3bkd and 2rlf) [33]. All bound ligands, ions, and water molecules were removed prior to mapping.

internal cavity and weaker hot spots on the outside of the channel (Figure 1). Why then is the inhibitor found only inside the pore in the X-ray structure, and only on the outside in the NMR experiment? This question is answered simply by comparing the sizes of the appropriate pockets in the two structures. In the X-ray structure the internal cavity is a large pocket that can easily accommodate an amantadine molecule. As expected, docking of amantadine to this structure places the lowest energy ligand clusters at this position [33]. We note that docked amantadine molecules can be observed at the weaker hot spot on the lipid-exposed outer surface of the channel at a location that binds rimantadine in the NMR structure. However, this pocket is shallow, and the average energy of amantadine binding there is much higher than the average energy in the pore [33]. By contrast, the largest pockets in the NMR structure are on the outside of the channel. The internal site with a volume of 85 Å^3 is ranked ninth by size, and it is too small to accommodate the bulky adamantane group. Indeed, the docking of amantadine to the NMR structure places ligands only at the outside binding pockets [33]. Because computational solvent mapping uses probes that are substantially smaller than amantadine, it still identifies the internal cavity as the most important hot spot.

Are two different amantadine binding modes and inhibition mechanisms possible?

The observation of the strongest hot spot in the pore for both X-ray and NMR structures indicates that amantadine first binds at this site, leading to inhibition by a pore-blocking mechanism [10,12]. However, the existence of additional hot spots on the outside of the channel suggests that the drug can bind on the outer surface, at least when the channel is closed. On the basis of the NMR structure, Schnell and Chou [11] proposed that the drug binds preferentially to, and thereby stabilizes, the closed state. They noted that amantadine action is faster at neutral pH, where the channel is mostly closed, than at low pH, where the open state is favored, in accord with closed-state stabilization but not with open-pore blocking [11,12]. Does the existence of both primary and secondary binding sites imply that inhibition might occur due to two different mechanisms? In fact, throughout the history of studying the M2 channel, numerous comments have suggested that one or the other mechanism leaves a number of observations unexplained. This suggestion was first made in an early paper by Pinto and Lamb [41], who listed four electrophysiological observations that, at least partly, contradicted amantadine binding within the pore and suggested the possibility of an allosteric inhibition mechanism. For example, they observed that the concentration of the drug required for half-maximal inhibition of current is greater when the channel is open (low pH) than when it is closed (high pH) [41]. Second, on the basis of the ssNMR data, Li *et al.* [18] noted that samples that have never been exposed to amantadine display a weak signal for the amantadine-bound conformation; similarly, they noted some evidence for the amantadine-free state even in the presence of amantadine at a concentration sufficient to saturate more than 99% of the sites. These findings hint at the possibility that amantadine shifts a conformational equilibrium between two states that are sampled in its absence. Third, although the amantadine-resistant mutants Ser31Asn and Ala30Thr do not bind amantadine, the mutants Val27Gly, Val27Ala, Ile27Ser and Ile27Thr are amantadine-resistant but they do bind amantadine [42]. Thus, according to these results, the virus might use two structural tactics to render a channel blocker ineffective. Fourth, the recent spectroscopic study reported by Manor *et al.* [22] found a large-scale conformational change in the channel structure when the pH was increased, suggesting that the channel pore is lined by a different set of residues in the open and closed states, and this can influence ligand binding [22].

The dual binding mechanism is compatible with the available functional data, which provide little information on the importance of binding at the exterior sites (Figure 2). The observation that Ser31Asn interferes with both mechanisms could explain why it underlies the primary resistance mutation [43,44]. By contrast, the Ser31Ala substitution, which does not lead to amantadine resistance, leaves both mechanisms unaffected. However, recent evidence shows that the outside binding cannot be solely responsible for inhibition. In the proposed NMR-derived external drug binding site, D44 makes a hydrogen
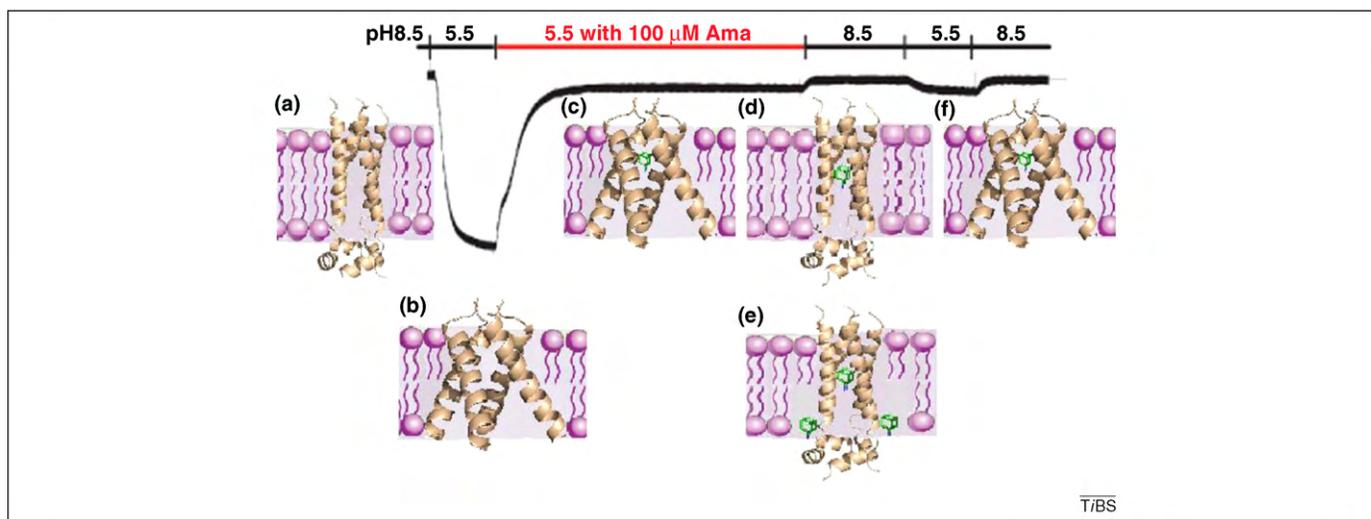
Figure 2. Compatibility of the dual binding mechanism with recording of surface currents through the M2 ion channel. A representative recording of surface currents through M2 channels expressed in oocytes of *Xenopus laevis* as the pH changes and amantadine is added, is shown (reproduced from Jing *et al.* [43] with permission). The experiment starts at pH 8.5. The pH is lowered to 5.5 to observe the opening of the channel, and amantadine is added in the fully open state, resulting in the observed inhibition (segment of recording shown in red). The pH is then increased to 8.5, lowered to 5.5, and increased to 8.5 again. The figure shows the most likely channel conformations and amantadine binding modes for each segment of the experiment. (a) At pH 8.5 the channel is closed. (b) The channel opens when the pH is reduced to 5.5. (c) After amantadine is added in the open state of the channel, the drug (shown in green) binds the most favorable site in the lumen of the pore, resulting in inhibition by the pore-blocking mode. The lipid-facing sites have substantially lower affinity for amantadine than the primary site, particularly in the open state of the channel when the helices splay relatively far apart near the C-terminus, and hence exterior binding is unlikely unless the amantadine/peptide ratio exceeds 1:4. Because the pore-blocking amantadine already provides inhibition, binding on the outside of the channel would not affect the current. (d) Increasing the pH closes the channel, at least to a certain degree, and most likely traps amantadine in the pore. (e) Because the external binding pockets become better defined when the channel is closed, at sufficiently high concentration amantadine binding is likely to also occur at the lipid-facing sites. (f) The pH is reduced to 5.5, but inhibition persists due to the bound inhibitor. We believe that this segment of the experiment provides little information on the effect of the allosteric inhibition due to the amantadine bound at the secondary sites. Although Schnell and Chou [11] suggest that the outside binding would contribute to maintaining the non-conductive state when the pH is lowered; at that point the system is already saturated by amantadine, most likely bound inside the pore, and any additional contribution would be negligible.

bond with amantadine. Jing *et al.* [43] showed that the M2 mutant channel with the substitution Asp44Ala is a functional and amantadine-sensitive ion channel. Furthermore, the Asp44Ala substitution into the influenza A virus did affect growth or sensitivity to amantadine [43].

Concluding remarks

Recently, a new ssNMR study [45] showed that the M2 channel in its closed conformation has both a high-affinity amantadine binding site inside the pore and four sites with lower affinity on the C-terminal protein surface, exactly as we predicted from mapping the X-ray and NMR structures [33]. Thus, our opinion that both sites exist has been validated. The new structure also shows that at the stoichiometric amantadine:peptide ratio of 1:4, the drug binds only to the lumenal site, and the exterior binding starts when it is in excess. The evidence that amantadine can bind in the closed channel [45] confirms that the NMR structure obtained by Schnell and Chou [11] is somehow distorted because its narrow pore is unable to accommodate the drug.

Although the new structure confirms that the primary binding site is in the pore, this does not exclude the potential existence of a dual inhibition mechanism. As we have discussed, electrophysiological recordings [43] neither refute nor confirm whether inhibitor binding to the secondary sites contributes to maintaining the non-conductive state when the pH is lowered (Figure 2). Although a number of observations reviewed here support the existence of an allosteric inhibition mechanism, accumulating evidence suggests that the secondary sites

have limited pharmacological significance in the wild type M2 channel [43]. However, assuming that the allosteric inhibition mechanism is confirmed, the secondary sites might become more important in drug-resistant mutants that are now found in over 97% of clinical isolates. Because neither the pore blocking nor the allosteric inhibition mechanism works in these mutants, the binding site in the pore does not necessarily have higher affinity, and hence both the internal and external sites are potential targets for the development of novel inhibitors that would evade drug resistance.

References

1 Helenius, A. (1992) Unpacking the incoming influenza-virus. *Cell* 69, 577–578
2 Sugrue, R.J. and Hay, A.J. (1991) Structural characteristics of the M2 protein of influenza A viruses: evidence that it forms a tetrameric channel. *Virology* 180, 617–624
3 Chizhmakov, I.V. *et al.* (1996) Selective proton permeability and pH regulation of the influenza virus M2 channel expressed in mouse erythroleukaemia cells. *J. Physiol.* 494, 329–336
4 Moffat, J.C. *et al.* (2008) Proton transport through influenza A virus M2 protein reconstituted in vesicles. *Biophys. J.* 94, 434–445
5 Tang, Y. *et al.* (2002) The gate of the influenza virus M2 proton channel is formed by a single tryptophan residue. *J. Biol. Chem.* 277, 39880–39886
6 Deyde, V.M. *et al.* (2007) Surveillance of resistance to adamantanes among influenza A(H3N2) and A(H1N1) viruses isolated worldwide. *J. Infect. Dis.* 196, 249–257
7 Bright, R.A. *et al.* (2006) Adamantane resistance among influenza A viruses isolated early during the 2005-2006 influenza season in the United States. *J. Am. Med. Assoc.* 295, 891–894

8 Hayden, F.G. (2006) Antiviral resistance in influenza viruses—implications for management and pandemic response. *N. Engl. J. Med.* 354, 785–788

9 Nishimura, K. *et al.* (2002) The closed state of a H$^+$ channel helical bundle combining precise orientational and distance restraints from solid state NMR. *Biochemistry* 41, 13170–13177

10 Stouffer, A.L. *et al.* (2008) Structural basis for the function and inhibition of an influenza virus proton channel. *Nature* 451, 596–599

11 Schnell, J.R. and Chou, J.J. (2008) Structure and mechanism of the M2 proton channel of influenza A virus. *Nature* 451, 591–595

12 Miller, C. (2008) Ion channels: coughing up flu's proton channels. *Nature* 451, 532–533

13 Kovacs, F.A. and Cross, T.A. (1997) Transmembrane four-helix bundle of influenza A M2 protein channel: structural implications from helix tilt and orientation. *Biophys. J.* 73, 2511–2517

14 Song, Z. *et al.* (2000) Transmembrane domain of M2 protein from influenza A virus studied by solid-state ^{15}N polarization inversion spin exchange at magic angle NMR. *Biophys. J.* 79, 767–775

15 Kovacs, F.A. *et al.* (2000) Helix tilt of the M2 transmembrane peptide from influenza A virus: an intrinsic property. *J. Mol. Biol.* 295, 117–125

16 Wang, J. *et al.* (2001) Structure of the transmembrane region of the M2 protein H$^+$ channel. *Protein Sci.* 10, 2241–2250

17 Hu, J. *et al.* (2007) Backbone structure of the amantadine-blocked trans-membrane domain M2 proton channel from influenza A virus. *Biophys. J.* 92, 4335–4343

18 Li, C. *et al.* (2007) Solid-state NMR characterization of conformational plasticity within the transmembrane domain of the influenza A M2 proton channel. *Biochim. Biophys. Acta* 1768, 3162–3170

19 Cady, S.D. *et al.* (2009) Structure of amantadine-bound M2 transmembrane peptide of influenza a in lipid bilayers from magic-angle-spinning solid-state NMR: the role of Ser31 in amantadine binding. *J. Mol. Biol.* 385, 1127–1141

20 Cady, S.D. and Hong, M. (2008) Amantadine-induced conformational and dynamical changes of the influenza M2 transmembrane proton channel. *Proc. Natl. Acad. Sci. U. S. A.* 105, 1483–1488

21 Hu, J. *et al.* (2007) The chemical and dynamical influence of the anti-viral drug amantadine on the M2 proton channel transmembrane domain. *Biophys. J.* 93, 276–283

22 Manor, J. *et al.* (2009) Gating mechanism of the influenza A M2 channel revealed by 1D and 2D IR spectroscopies. *Structure* 17, 247–254

23 Yi, M. *et al.* (2009) Conformational heterogeneity of the M2 proton channel: a structural model for channel activation. *Proc. Natl. Acad. Sci. U. S. A.* 106, 13311–13316

24 Leonov, H. and Arkin, I.T. (2009) Structure and dynamics of the influenza A M2 channel: a comparison of three structures. *J. Mol. Model.* 15, 1317–1328

25 Khurana, E. *et al.* (2009) Molecular dynamics calculations suggest a conduction mechanism for the M2 proton channel from influenza A virus. *Proc. Natl. Acad. Sci. U. S. A.* 106, 1069–1074

26 Duong-Ly, K.C. *et al.* (2005) The conformation of the pore region of the M2 proton channel depends on lipid bilayer environment. *Protein Sci.* 14, 856–861

27 Pinto, L.H. and Lamb, R.A. (2007) Controlling influenza virus replication by inhibiting its proton channel. *Mol. Biosyst.* 3, 18–23

28 Im, W. *et al.* (2003) An implicit membrane generalized Born theory for the study of structure, stability, and interactions of membrane proteins. *Biophys. J.* 85, 2900–2918

29 Chou, J.J. *et al.* (2002) Micelle-induced curvature in a water-insoluble HIV-1 Env peptide revealed by NMR dipolar coupling measurement in stretched polyacrylamide gel. *J. Am. Chem. Soc.* 124, 2450–2451

30 Chou, J.J. *et al.* (2004) Characterization of phospholipid mixed micelles by translational diffusion. *J. Biomol. NMR* 29, 299–308

31 Poget, S.F. and Girvin, M.E. (2007) Solution NMR of membrane proteins in bilayer mimics: small is beautiful, but sometimes bigger is better. *Biochim. Biophys. Acta* 1768, 3098–3106

32 Fernández, C. (2002) Lipid-protein interactions in DHPC micelles containing the integral membrane protein OmpX investigated by NMR spectroscopy. *Proc. Natl. Acad. Sci. U. S. A.* 99, 13533–13537

33 Chuang, G-Y. *et al.* (2009) Binding hot spots and amantadine orientation in the influenza A virus M2 proton channel. *Biophys. J.* 97, 2846–2853

34 Landon, M.R. *et al.* (2007) Identification of hot spots within druggable binding sites of proteins by computational solvent mapping. *J. Med. Chem.* 50, 1231–1240

35 Brenke, R. *et al.* (2009) Fragment-based identification of druggable "hot spots" of proteins using Fourier domain correlation techniques. *Bioinformatics* 25, 621–627

36 Hajduk, P.J. *et al.* (2005) Druggability indices for protein targets derived from NMR-based screening data. *J. Med. Chem.* 48, 2518–2525

37 Mattos, C. and Ringe, D. (1996) Locating and characterizing binding sites on proteins. *Nat. Biotechnol.* 14, 595–599

38 Laurie, A.T.R. and Jackson, R.M. (2005) Q-SiteFinder: an energy-based method for the prediction of protein–ligand binding sites. *Bioinformatics* 21, 1908–1916

39 Chew, C.F. (2008) Distribution and dynamics of adamantanes in a lipid bilayer. *Biophys. J.* 95, 5627–5636

40 Li, C. *et al.* (2008) Solid-state NMR and MD simulations of the antiviral drug amantadine solubilized in DMPC bilayers. *Biophys. J.* 94, 1295–1302

41 Pinto, L.H. and Lamb, R.A. (1995) Understanding the mechanism of action of the anti-influenza virus drug amantadine. *Trends Microbiol.* 3, 271

42 Astrahan, P. *et al.* (2004) A novel method of resistance for influenza against a channel-blocking antiviral drug. *Proteins: Struct. Funct. Bioinformatics* 55, 251–257

43 Jing, X. *et al.* (2008) Functional studies indicate amantadine binds to the pore of the influenza A virus M2 proton-selective ion channel. *Proc. Natl. Acad. Sci. U. S. A.* 105, 10967–10972

44 Pielak, R.M. *et al.* (2009) Mechanism of drug inhibition and drug resistance of influenza A M2 channel. *Proc. Natl. Acad. Sci. U. S. A.* 106, 7379–7384

45 Cady, S.D. *et al.* (2010) Structure of the amantadine binding site of influenza M2 proton channels in lipid bilayers. *Nature* 463, 689–692